Supporting Information

FIGURE S1. **Confirmation of the specificity of anti-CPD and -SIRT1 antibodies for proximity ligation.** Proximity ligation assay (PLA) using *A*, SIRT1-CPD antibodies, *B*, only single SIRT1, *C*, only single CPD antibodies or *D*, no amplification controls. A375 melanoma cells were exposed to UVB (10 J/m^2) and allowed to repair for 1 h or mock treated. Green detection events signify juxtaposition between SIRT1 and CPD in maximum intensity projection images. Nuclei were stained with DAPI (blue). Note: the omission of each primary antibody or all primary antibodies did not generate any non-specific signals.

FIGURE S2. **Expression of kinase-deficient forms of ATR diminish UV-induced Chk1 phosphorylation.** A375 melanoma cells were either not transfected or transfected with ATR-WT, ATR-kinase dead (KD) or ATR-P2445L and exposed to UVB (10 J/m^2) or mock treated. At 1hr post-UV lysates were immunoblotted with anti-Chk1 and anti-Chk1-pS345.

FIGURE S3. **SIRT1 is localized to damage DNA in an ATR-dependent manner but is not directly phosphorylated by ATR.** *A,* A375 melanoma cells were treated with vehicle or either 10μM of the following inhibitors for 30 min, ATRi (VE-821), ATMi (Ku-55933) or DNA-PKi (KU-7026). Cells were exposed to UVB (10 J/m^2) or mock treated and allowed to repair for 1 h. Chromatin extract was used to immunoblot with anti-SIRT1. The levels of H2A was used as a loading control. *B*, Immunoprecipitation of SIRT1 with anti-SIRT1 antibodies in A375 cells either mock treated or 1h post UVB exposure (10 J/m^2). Lysates were immunoblotted with an ATR/ATM phosphorylation-specific antibody that detects phosphorylated SQ/TQ motifs. The phosphorylation of Chk1 by ATR was used as a positive control. Immunoblot inputs represent 10% of total cellular lysate

FIGURE S4. **Mutations in ATR and SIRT1 are associated with a higher mutational burden in melanoma.** Comparison of the total mutational burden in primary melanomas either containing *A*, mutated ATR versus a wild-type ATR or *B*, mutated SIRT1 versus wild-type SIRT1. Comparison of the mutational burden in primary melanomas at CC-TT sites either containing *C*, mutated ATR versus a wild-type ATR or *D*, mutated SIRT1 versus wild-type SIRT1. All analyses were performed by Wilcoxon rank sum tests using The Cancer Genome Atlas human skin cutaneous melanoma dataset (n=470). $P<0.05$ was considered as statistically significant. Note that all values in the figure were added by 1 before taking the log-transformation due to the presence of zeros.

FIGURE S5. **cAMP enhances SIRT1 activity.** *A,* A375 melanoma cells were pretreated with vehicle or forskolin (10 μM) for 30 min and mock treated or UVB irradiated (10 J/m^2) as indicated. In addition, cells were either treated with 10μM of H-89, EX-527 or VE-821 as indicated. At 1hr post-damage, cell lysates were used to measure SIRT1 activity using a fluorophore peptide containing an acetylated lysine, as described in the manufacturer's protocol. Values not sharing a common letter were significantly different as determined by one-way ANOVA; $p \leq 0.05$.

FIGURE S6. **Basal cAMP levels impact DNA repair, XPA-deacetylation and XPA-pS196 levels.** *A*, basal levels of cAMP in A375 cells were measured with a combination of 10μM of H-89 (PKAi) and 2′,5′-Dideoxyadenosine (ACi). *B*, A375 cells were pretreated with vehicle, forskolin (10 μM) or a combination of 10μM of H-89 (PKAi) and 2′,5′-Dideoxyadenosine (ACi) for 30 min and mock treated or UVB irradiated (10 J/m^2). CPD levels were measured at 24 and 48 h post-damage using anti-CPD antibodies. The * on the treated (either forskolin treated or PKAi and ACi treated) cells repair kinetics indicate a significant difference in amount of damage at the indicated time point compared to the amount of damage in non-treated cells (vehicle-treated). *$p \leq 0.05$. C, A375 cells were pretreated with vehicle, forskolin (10 μM) or a combination of 10μM of H-89 (PKAi) and 2′,5′-Dideoxyadenosine (ACi) for 30 min and mock treated or UVB irradiated (10 J/m^2). Co-IP with anti-acetylation (Ac-K) antibody and immunoblot with anti-XPA antibody was performed. Input represents 10% of total cellular level. D, A375 cells were pretreated with

vehicle, forskolin (10 μM) or a combination of 10μM of H-89 (PKAi) and 2′,5′-Dideoxyadenosine (ACi) for 30 min and mock treated or UVB irradiated (10 J/m^2). Nuclear levels of XPA-pS196 were determined by immunoblotting.

FIGURE S7. **UV and cAMP promote the XPA-ATR interaction.** *A*, A375 melanoma cells were pretreated with vehicle or forskolin (10 μM) and mock treated or UVB irradiated (10 J/m^2). Proximity ligation assay of the ATR-XPA interaction in A375 melanoma cells at 1 h after UVB (10 J/m^2) or mock treatment. PLA was performed with anti-ATR and anti-XPA antibodies. Green detection events signify juxtaposition between ATR and XPA in maximum intensity projection images. Nuclei were stained with DAPI (blue). Bar represents 50 μm.

FIGURE S8. **Confirmation of the specificity of anti-ATR and -XPA antibodies for proximity ligation.** Proximity ligation assay (PLA) using *A*, ATR-XPA antibodies, *B*, only single ATR, *C*, only single XPA antibodies or *D*, no amplification controls. A375 melanoma cells were exposed to UVB (10 J/m^2) and allowed to repair for 1 h or mock treated. Green detection events signify juxtaposition between SIRT1 and CPD in maximum intensity projection images. Nuclei were stained with DAPI (blue). Note: the omission of each primary antibody or all primary antibodies did not generate any non-specific signals.

FIGURE S9. **Acetylated-lysine 215 is deacetylated by SIRT1 in a cell free system**. *A*, Recombinant SIRT1 together with NAD, as described in experimental procedures, were incubated with 10 μM peptide (RQENRERMK(AcK)QRKF) containing K215 of XPA and surrounding residues (with other lysine residues modified to arginine). The peptide was acetylated by CREB, as described in experimental procedures. Deacetylation was measured using anti-acetyl-lysine antibody coupled with fluorescence detection. B, Lysine 215 is highly conserved.

FIGURE S10. **XPA-S196 enhances SIRT1 protein stability**. XPA CRISPR/Cas9 deleted A375 melanoma cells were complemented with either *A*, XPA-WT or XPA-S196A. *B*, XPA CRISPR/Cas9 deleted A375 melanoma cells expressing either XPA-WT or XPA-S196A were exposed to UVB (10 J/m^2) and allowed to repair for the indicated times in the presence of cycloheximide (20 μg/ml). Nuclear extracts were probed with anti-SIRT1 levels and immunoblot. Equal loading was confirmed by probing for Lamin B1.

FIGURE S11. **XPA acetylation mimetics K63Q, K67Q and K215Q interfere with cAMP-mediated enhancement of NER.** *A*, Protein expression levels of XPA in CRISPR-edited A375 cells and subsequent expression of XPA plasmids. XPA CRISPR/Cas9 deleted A375 melanoma cells complemented with either *B*, XPA-WT, *C*, XPA-K63Q, *D*, XPA-K67Q, *E*, XPA-K215Q, *F*, XPA-K63/67/215/215Q, *G*, XPA-K63/67/215/215Q-S196A or *H*, XPA-K63/67/215/215Q-S196D were pretreated with vehicle or forskolin (10 μM) for 30 min and mock treated or UVB irradiated (10 J/m^2). CPD levels were measured at 24 and 48 h post-damage using anti-CPD antibodies. The red * (forskolin) on the mutant XPA graphs indicate a significant difference in amount of damage at the indicated time point compared to the amount of damage in the XPA-wild-type cells (Panel A). *$p \leq 0.05$.

FIGURE S12. The **XPA acetylation mimetic K63Q/K67Q/K215Q/S196D bypasses SIRT1 but not ATR.** XPA CRISPR/Cas9 deleted A375 melanoma cells complemented with either *A*, XPA-WT or XPA-K63Q/K67Q/K215Q/S196D were pretreated with either *A*, vehicle, *B*, EX-527 (10 μM) or ,*C*, VE-821 (10 μM) for 30 min and UVB irradiated (10 J/m^2). CPD levels were measured at 24 and 48 h post-damage using anti-CPD antibodies.

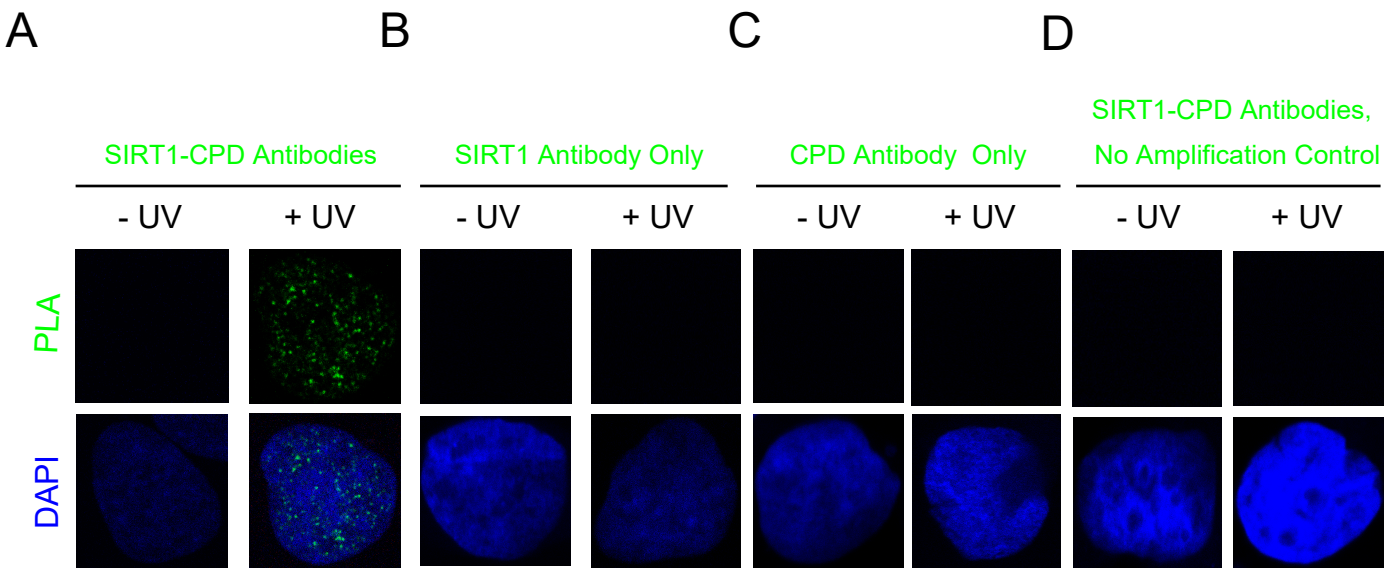

Jarrett et al, Figure S1

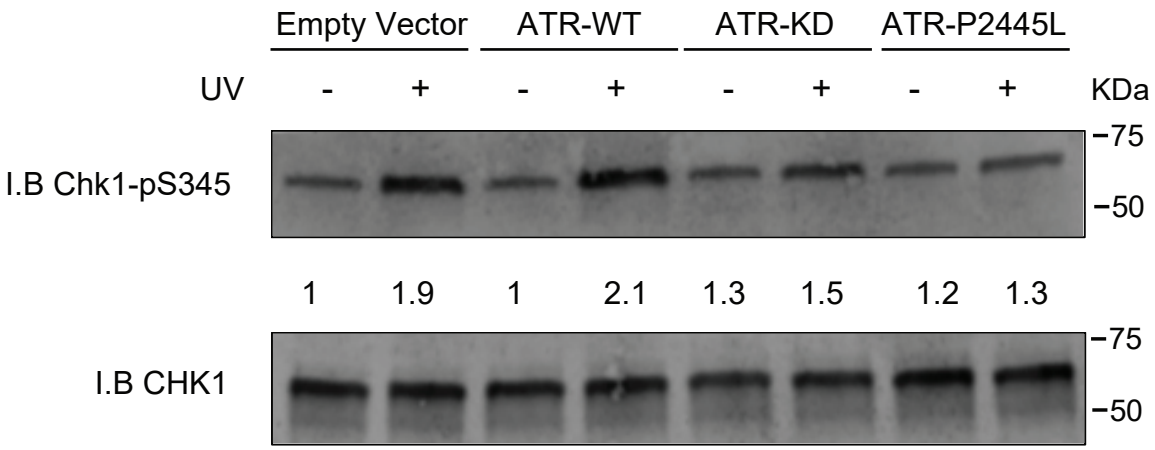

Jarrett et al, Figure S2

A

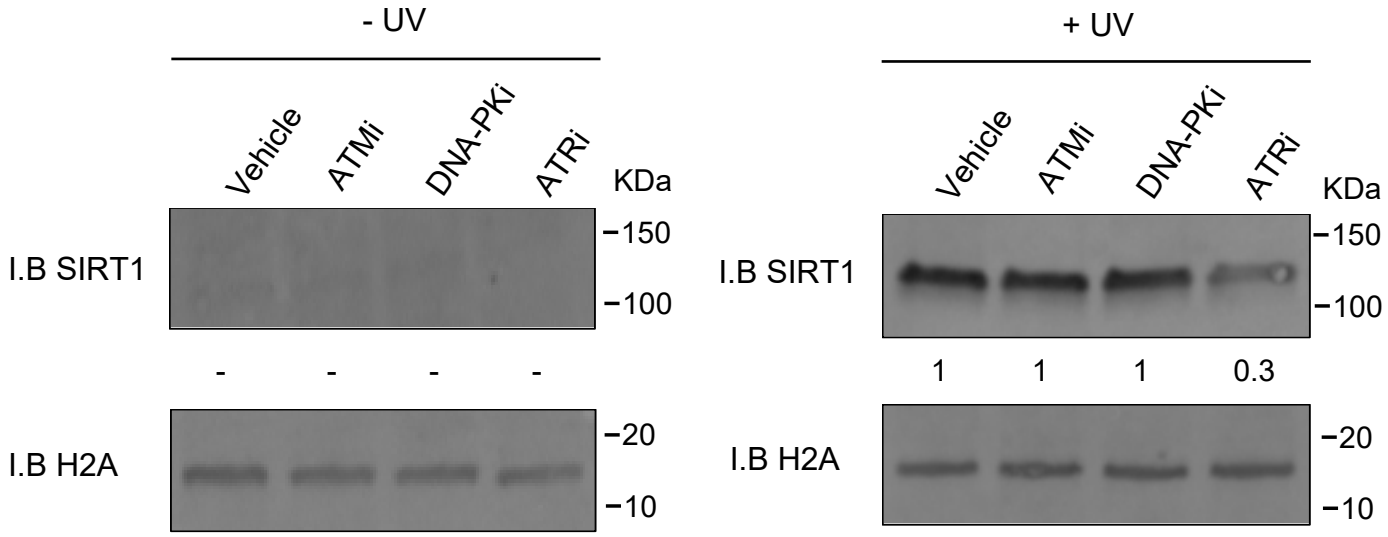

B

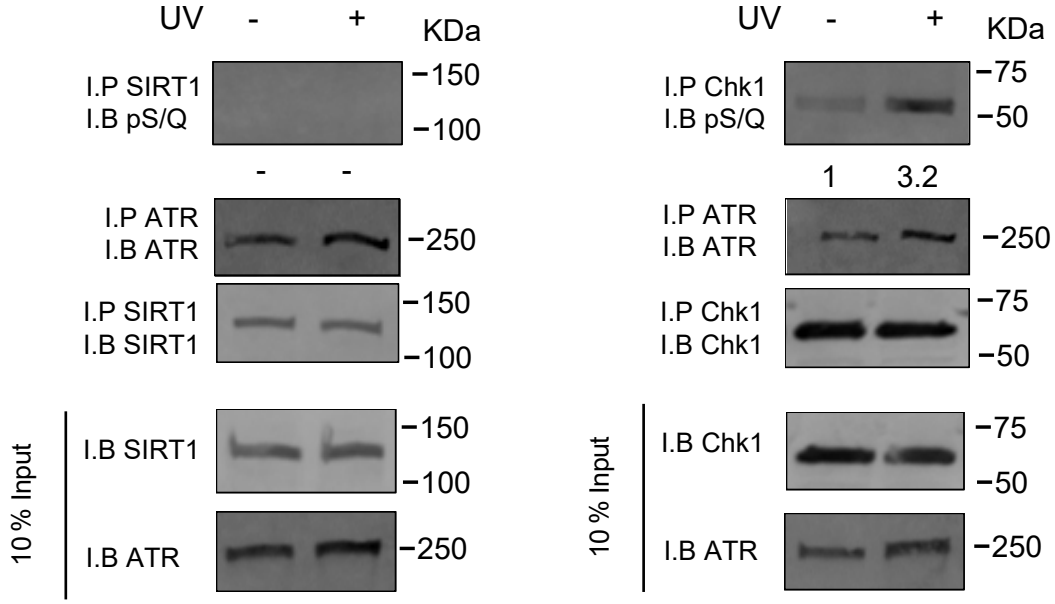

Jarrett et al, Figure S3

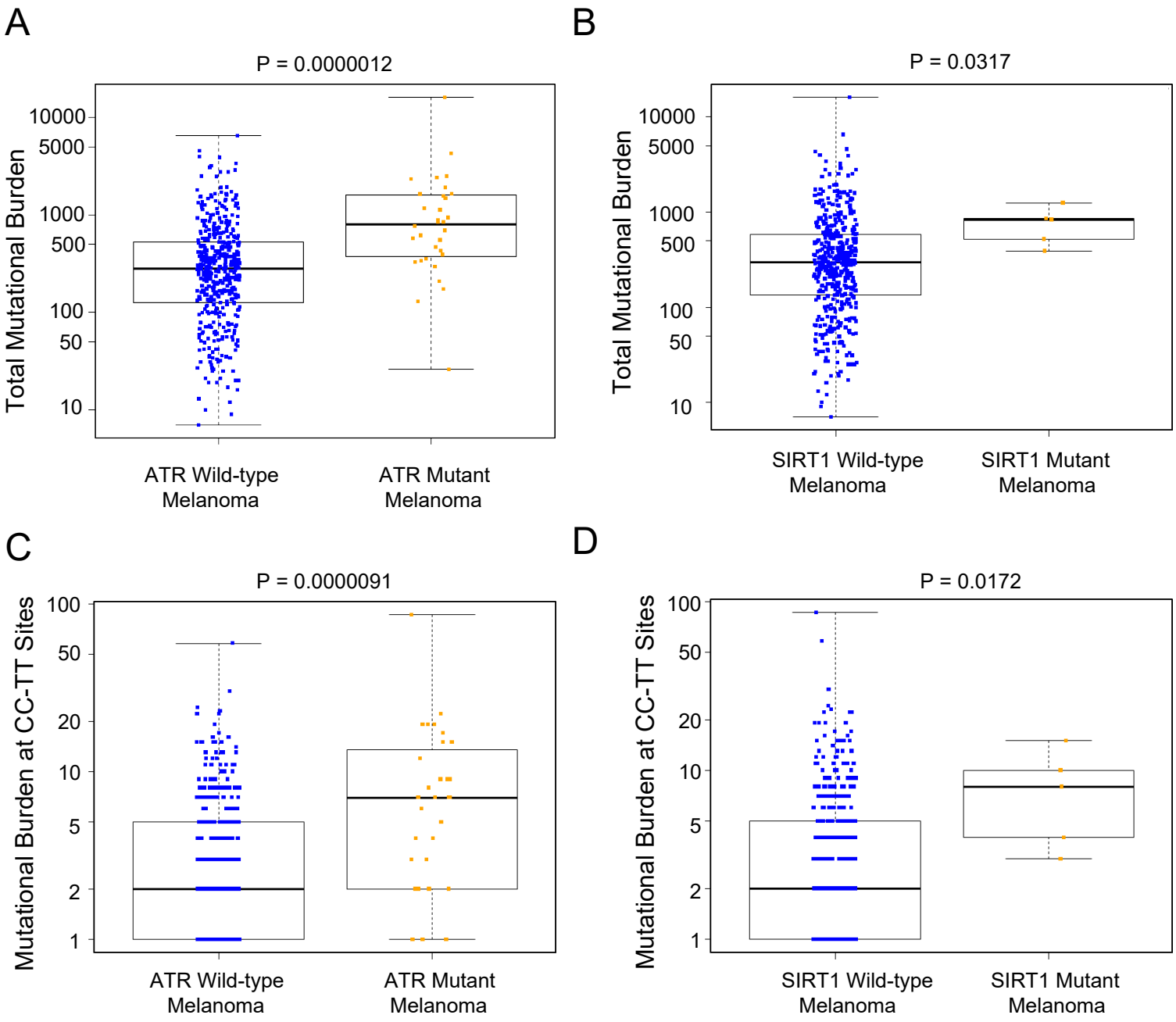

Jarrett et al, Figure S4

A

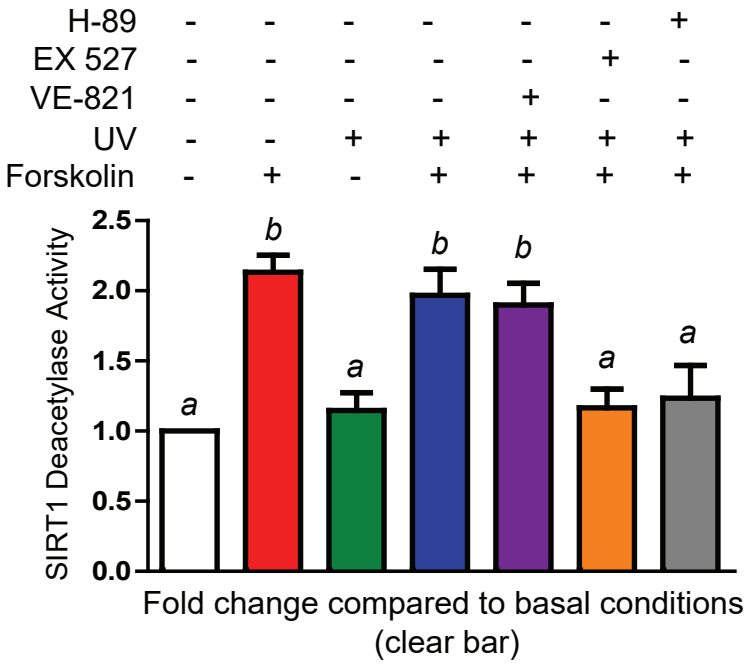
H-89 - - - - - - +
EX 527 - - - - - + -
VE-821 - - - - + - -
UV - - + + + + +
Forskolin - + - + + + +
SIRT1 Deacetylase Activity
2.5
2.0
1.5
1.0
0.5
0.0
a
b
a
b
b
a
a
Fold change compared to basal conditions
(clear bar)

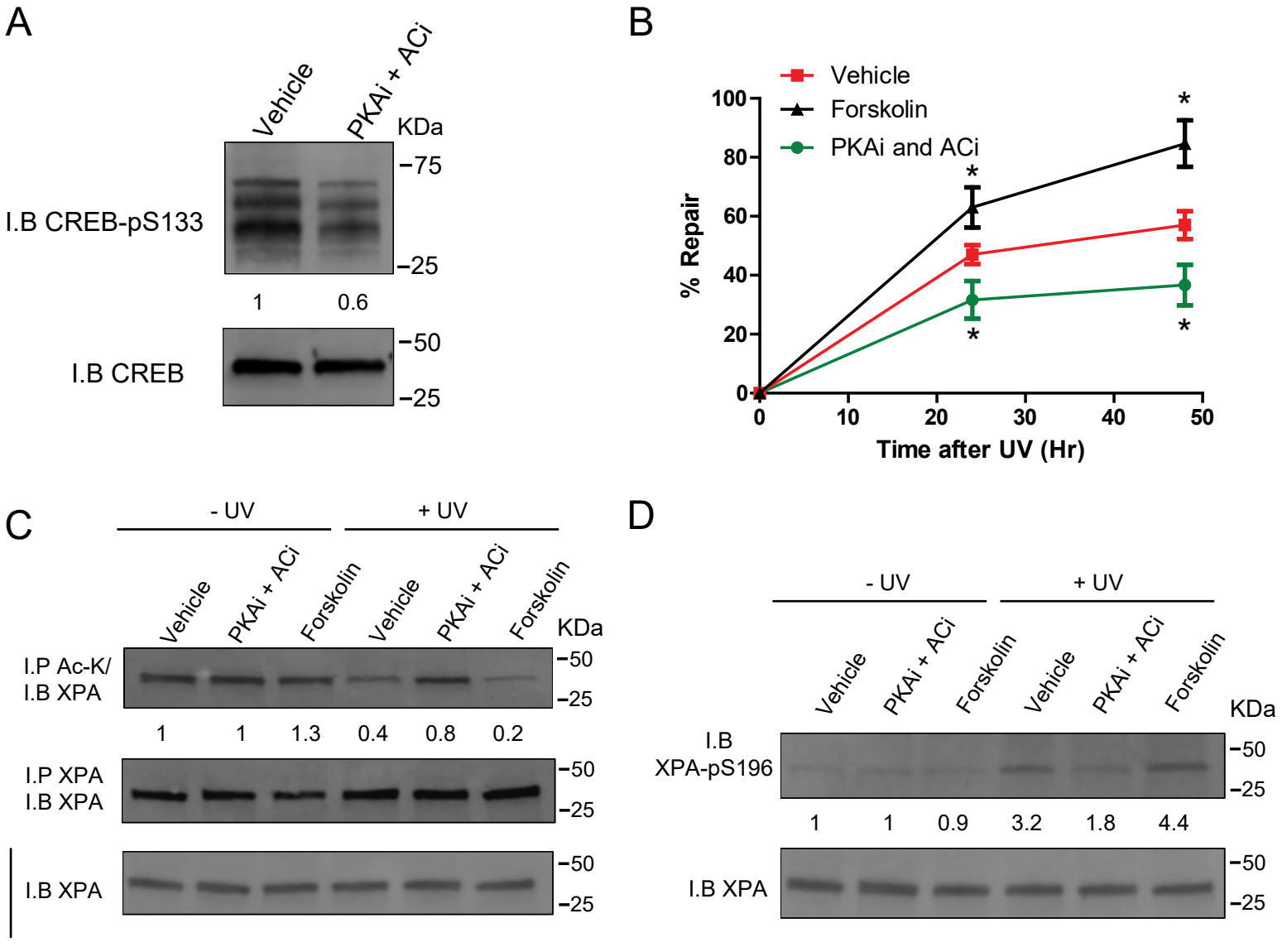

Jarrett et al, Figure S6

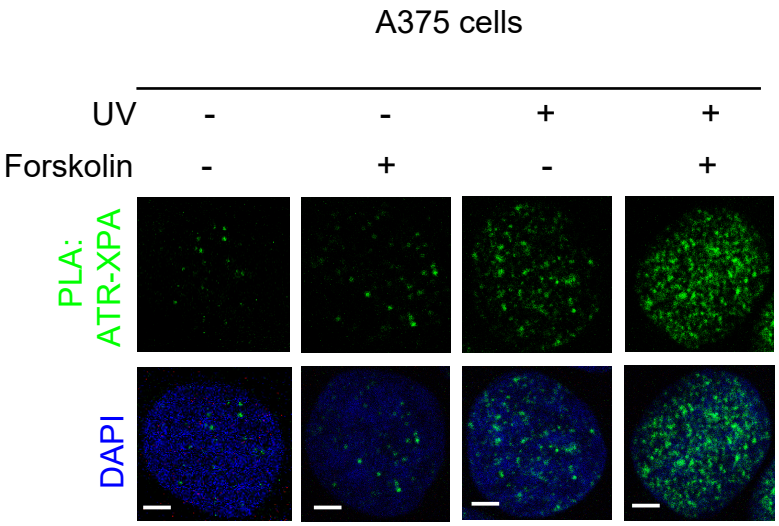

Jarrett et al, Figure S7

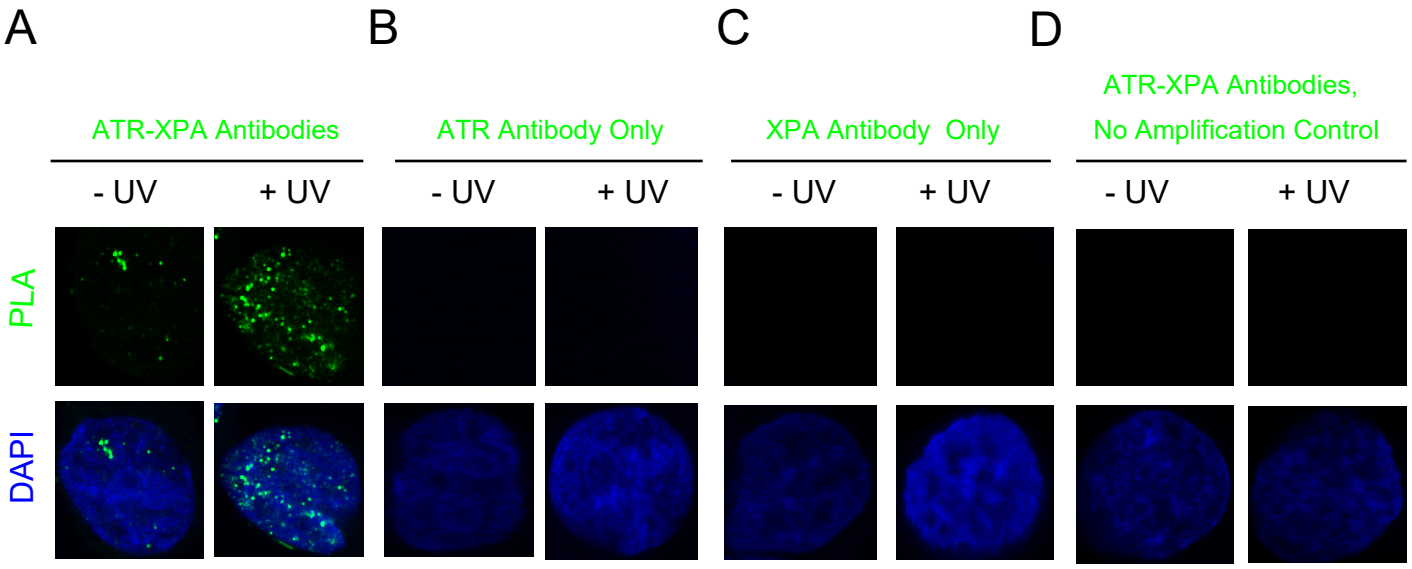

Jarrett et al, Figure S8

A

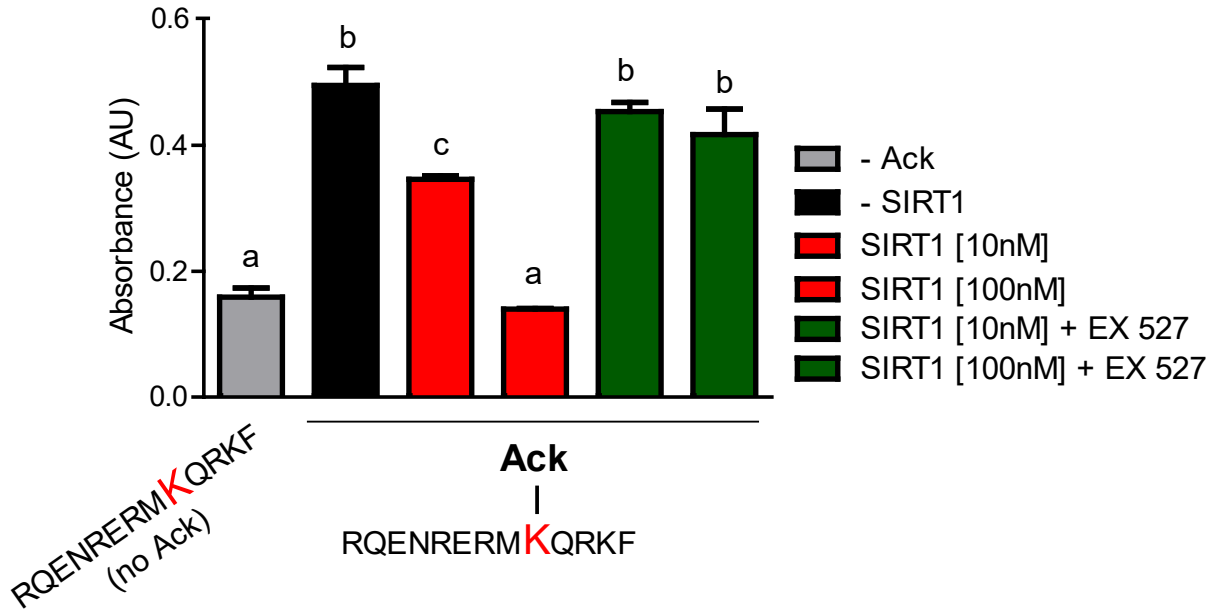

B

	215
Homo sapiens (human)	QENREKMKQKKFDKK
Pan troglodytes (common chimpanzee)	QENREKMKQKKFDKK
Equus caballus (horse)	QENREKMKQKKFDKK
Bos taurus (cow)	QKNREKMKQKKFDKK
Canis lupus (gray wolf)	QENREKMKQKKFDKK
Sus scrofa (wild boar)	QKNREKMKQKKFDKK
Rattus norvegicus (brown rat)	QENREKMKQKKFDKK
Mus musulus (house mouse)	QENREKMKQKKFDKK
Oryctolagus cuniculus (European rabbit)	QENREKMKQKKFDKK
Condylura cristata (star-nosed mole)	QENREKMKQKKFDKK
Gallus gallus (chicken)	RDSREKMKQKRFDKK
Xenopus laevus (African clawed frog)	KDNRDKMKQKKFDKK
Drosophila melanogaster (fruit fly)	RKYNKKMKQLRMEVR

Jarrett et al, Figure S9

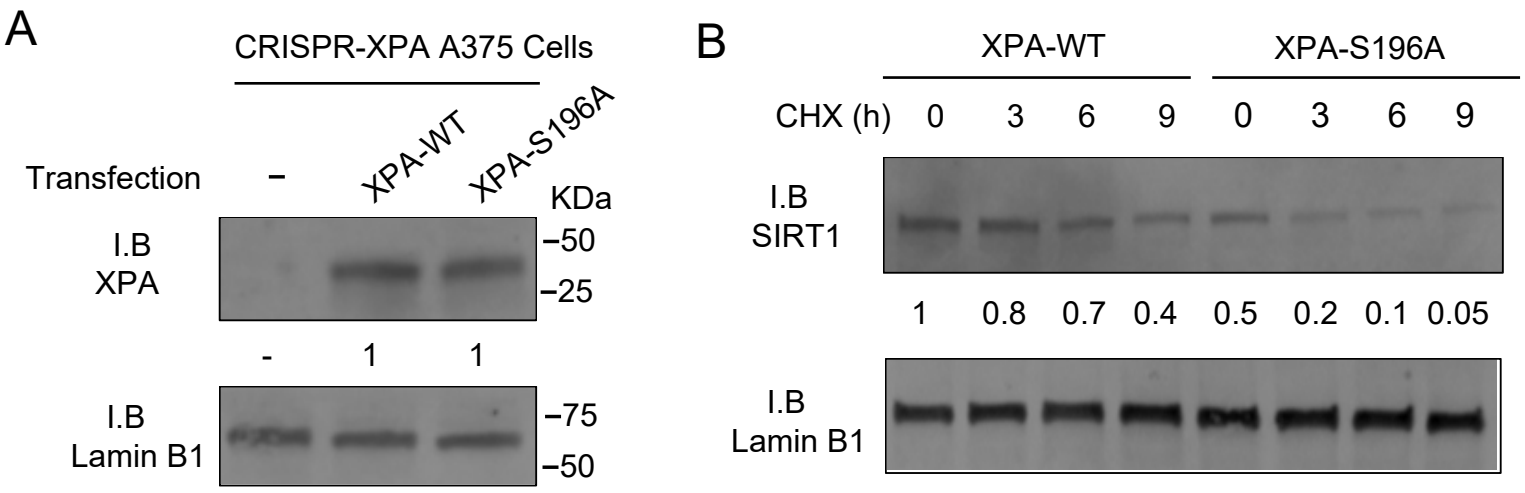

Jarrett et al, Figure S10

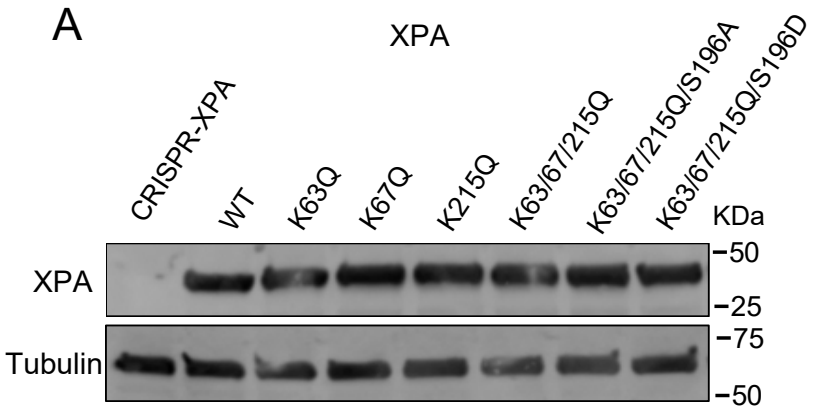

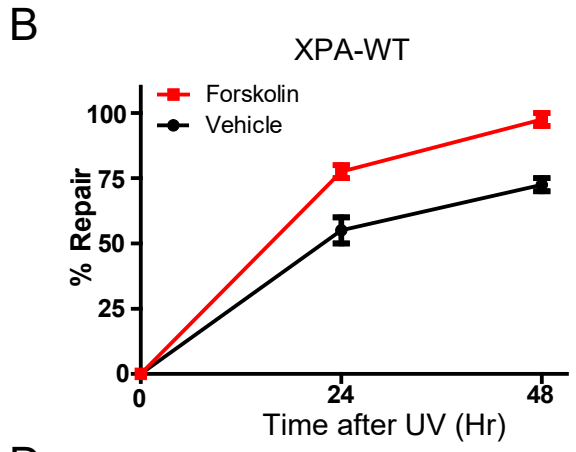

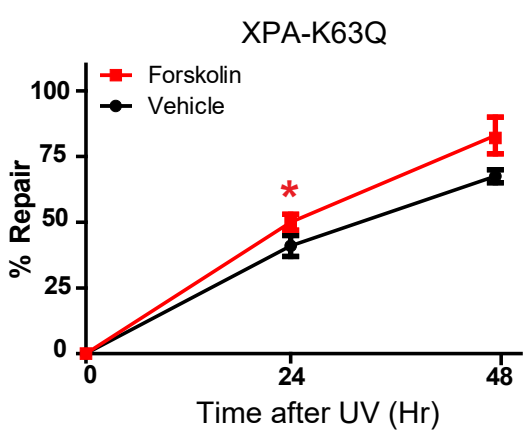

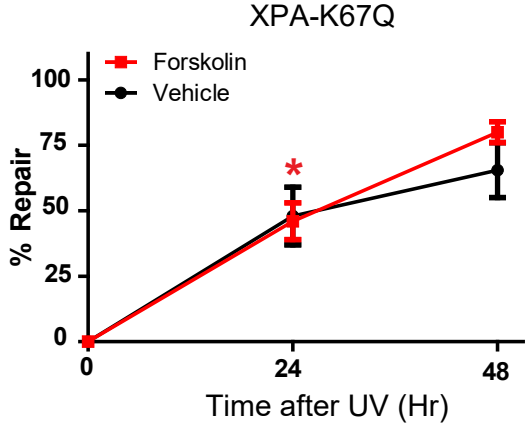

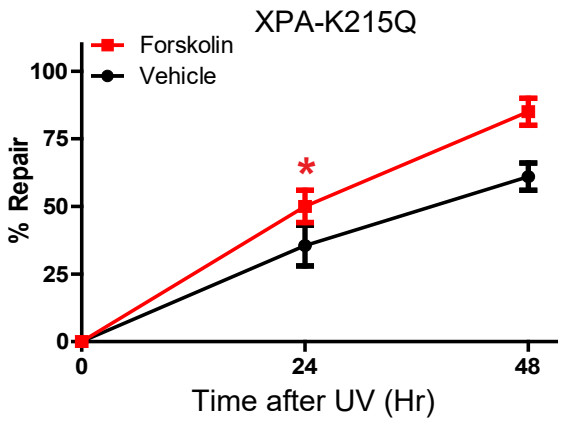

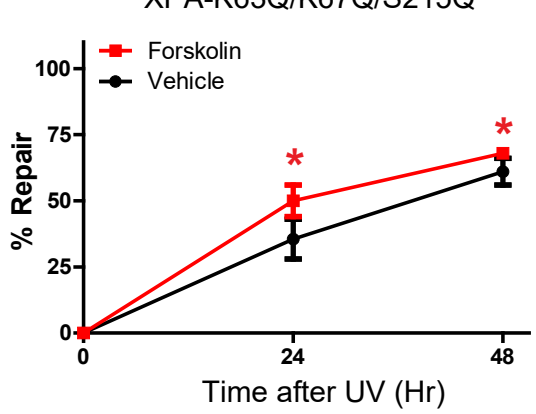

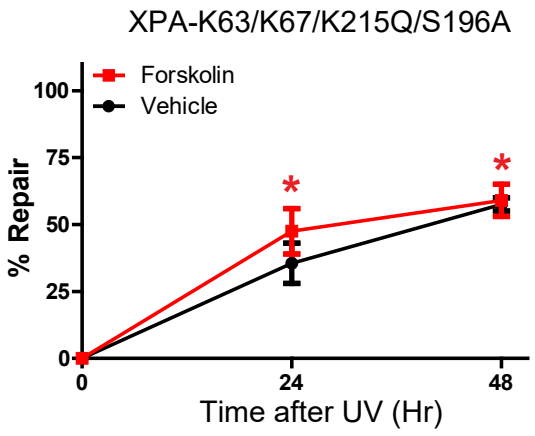

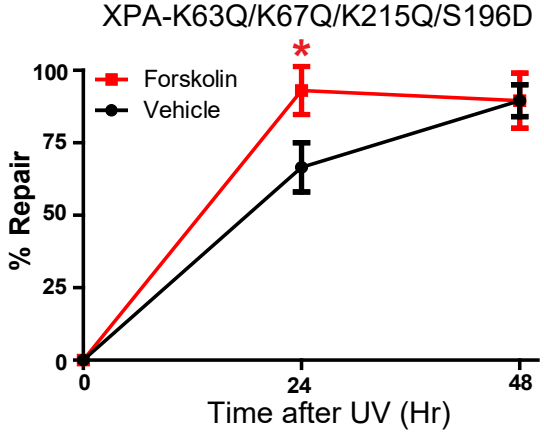

Jarrett et al, Figure S11

A

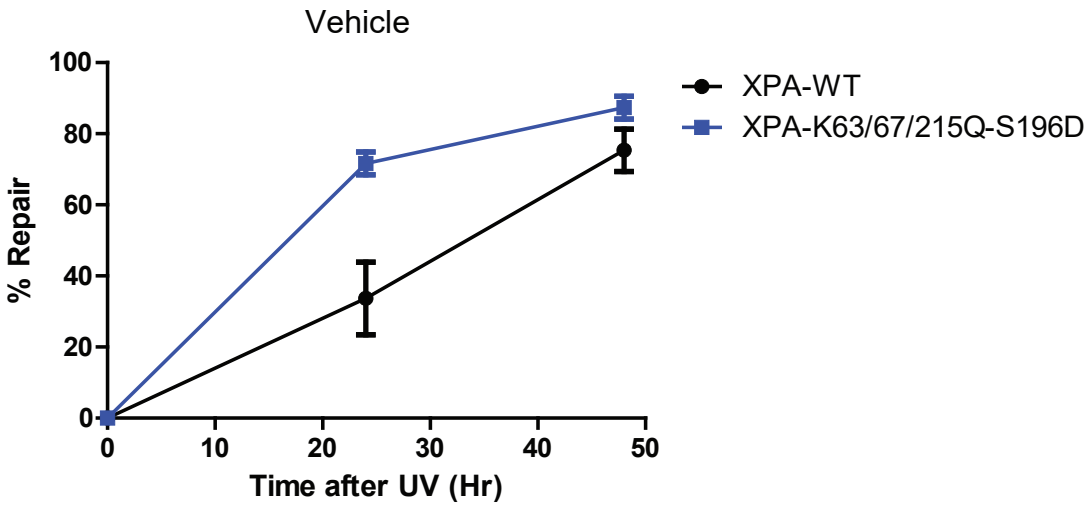

B

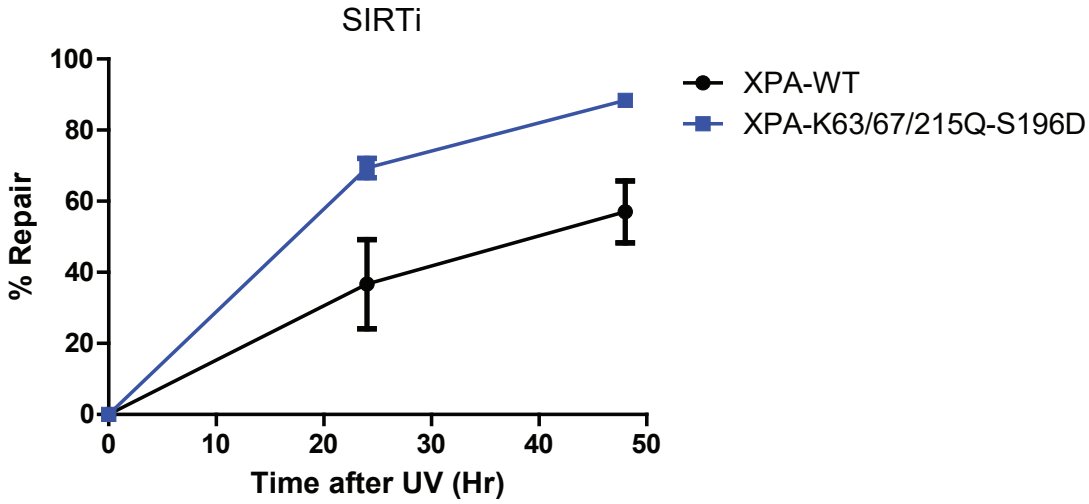

C

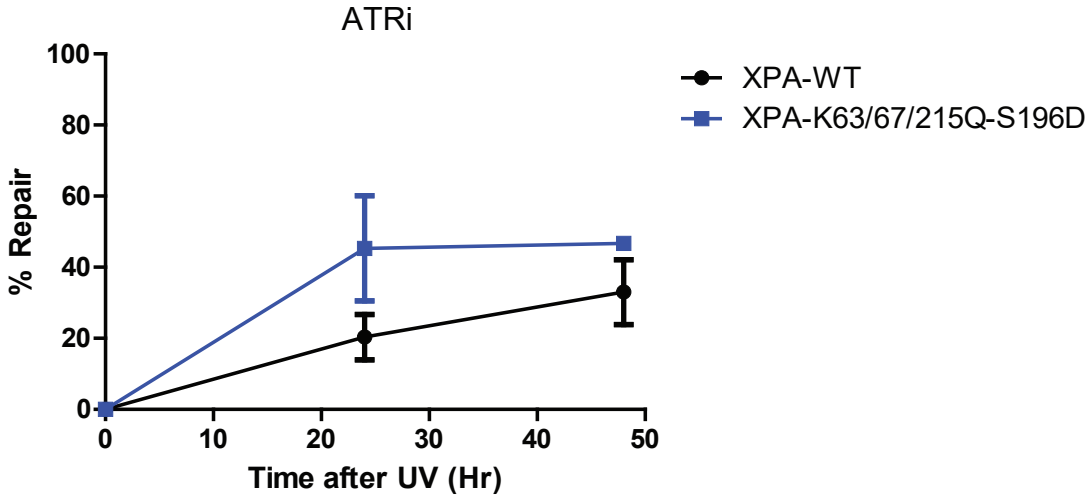

Jarrett et al, Figure S12